Inorganic Chemistry
Article

Inorg. Chem. **2010**, *49*, 11581–11586 **11581**
DOI: 10.1021/ic1017467

New Three-Dimensional Porous Metal Organic Framework with Tetrazole Functionalized Aromatic Carboxylic Acid: Synthesis, Structure, and Gas Adsorption Properties

Shu-Ming Zhang,[†,‡] Ze Chang,[†] Tong-Liang Hu,[†] and Xian-He Bu*[,†]

[†]*Department of Chemistry, Tianjin Key Laboratory of Metal and Molecule-based Material Chemistry, Nankai University, Tianjin 300071, China, and* [‡]*School of Chemical Engineering and Technology, Hebei University of Technology, Tianjin 300130, China*

Received August 27, 2010

5-(1H-Tetrazol-1-yl)isophthalic acid (H_2**L**) reacts with Cu(II) ion forming a new metal−organic framework $\{[Cu\mathbf{L}]\cdot DMF\cdot H_2O\}_\infty$ (**1**) (DMF = *N*,*N*-dimethylformamide), with a rutile-related type net topology. Compound **1** possesses a 3D structure with 1D channels that can be desolvated to yield a microporous material. Adsorption properties (N_2, H_2, O_2, CO_2, and CH_4) of the desolvated solid [Cu**L**] (**1a**) have been studied, and the results exhibit that **1a** possesses fairly good capability of gas sorption for N_2, H_2, O_2, and CO_2 gases, with high selectivity ratios for O_2 over H_2 at 77 K and CO_2 over CH_4 at 195, 273, and 298 K. Furthermore, **1a** has excellent O_2 uptake at 77 K and a remarkably high quantity of adsorption for CO_2 at room temperature (298 K) and atmospheric pressure, suggesting its potential applications in gas separation or purification.

Introduction

The rational design and construction of metal−organic crystalline materials has been a hot topic for many years, due to not only their fascinating structures and topologies but also their specific or multifunctional properties.[1] Recently, increasing attention has been attracted to the porous metal organic frameworks (MOFs), which possess rich structural chemistry and excellent gas sorption properties.[2] Porous MOFs constructed by the metal ions or metallic clusters linked with organic linkers have an advantage in that their porous surface can be varied to a greater extent than in other porous materials,[3b] exhibiting particularly potential applications in catalysis, ion exchange, purification, gas storage, and gas separation.[3,4] As an important class of building block, the metal motifs, such as dinuclear, trinuclear, and even higher-nuclear clusters, have been used as secondary building units (SBUs) to construct robust and highly porous MOFs, for their stability and specific conformation that make the design and prediction of the resulting architectures simple and easy.[4a,5] During our ongoing effort to construct porous MOFs, we chose 5-(1H-tetrazol-1-yl)isophthalic acid (H_2**L**)

*To whom correspondence should be addressed. E-mail: buxh@nankai.edu.cn. Fax: +86-22-23502458. Tel: +86-22-23502809.

(1) For examples, see (a) Shimomura, S.; Higuchi, M.; Matsuda, R.; Yoneda, K.; Hijikata, Y.; Kubota, Y.; Mita, Y.; Kim, J.; Takata, M.; Kitagawa, S. *Nat. Chem.* **2010**, *2*, 633. (b) Zeng, Y.-F.; Hu, X.; Liu, F.-C.; Bu, X.-H. *Chem. Soc. Rev.* **2009**, *38*, 469. (c) Jang, J.-J.; Li, L.; Yang, T.; Kuang, D.-B.; Wang, W.; Su, C.-Y. *Chem. Commun.* **2009**, 2387. (d) Cairns, A. J.; Perman, J. A.; Wojtas, L.; Kravtsov, V.Ch.; Alkordi, M. H.; Eddaoudi, M.; Zaworotko, M. J. *J. Am. Chem. Soc.* **2008**, *130*, 1560. (e) Hoeben, F. J. M.; Jonkheijm, P.; Meijer, E. W.; Schenning, A. P. H. J. *Chem. Rev.* **2005**, *105*, 1491. (f) Bu, X.-H.; Tong, M.-L.; Chang, H.-C.; Kitagawa, S.; Batten, S. R. *Angew. Chem., Int. Ed.* **2004**, *43*, 192.

(2) For examples, see (a) Li, J.-R.; Kuppler, R. J.; Zhou, H.-C. *Chem. Soc. Rev.* **2009**, *38*, 1477. (b) Chun, H.; Seo, J. *Inorg. Chem.* **2009**, *48*, 9980. (c) Liu, Y. L.; Kravtsov, V. C.; Eddaoudi, M. *Angew. Chem., Int. Ed.* **2008**, *47*, 8446. (d) Bünzli, J.-C. G. *Acc. Chem. Res.* **2006**, *39*, 53. (e) Pan, L.; Parker, B.; Huang, X. Y.; Olson, D. H.; Lee, J. Y.; Li, J. *J. Am. Chem. Soc.* **2006**, *128*, 4180.

(3) (a) Cheon, Y. E.; Suh, M. P. *Chem.Commun.* **2009**, 2296. (b) Thomas, K. M. *Dalton Trans.* **2009**, 1487. (c) Férey, G. *Chem. Soc. Rev.* **2008**, *37*, 191. (d) Wang, B.; Cote, A. P.; Furukawa, H.; O' Keeffe, M.; Yaghi, O. M. *Nature* **2008**, *453*, 207. (e) Shimomura, S.; Horike, S.; Matsuda, R.; Kitagawa, S. *J. Am. Chem. Soc.* **2007**, *129*, 10990. (f) Collins, D. J.; Zhou, H.-C. *J. Mater. Chem.* **2007**, *17*, 3154. (g) Lin, X.; Blake, A. J.; Wilson, C.; Sun, X. Z.; Champness, N. R.; George, M. W.; Hubberstey, P.; Mokaya, R.; Schröder, M. *J. Am. Chem. Soc.* **2006**, *128*, 10745. (h) Matsuda, R.; Kitaura, R.; Kitagawa, S.; Kubota, Y.; Belosludov, R. V.; Kobayashi, T. C.; Sakamoto, H.; Chiba, T.; Takata, M.; Kawazoe, Y.; Mita, Y. *Nature* **2005**, *436*, 238.

(4) (a) Lee, Y.-G.; Moon, H. R.; Cheon, Y. E.; Suh, M. P. *Angew. Chem., Int. Ed.* **2008**, *47*, 7741. (b) Li, J.-R.; Tao, Y.; Yu, Q.; Bu, X.-H.; Sakamoto, H.; Kitagawa, S. *Chem.−Eur. J.* **2008**, *14*, 2771. (c) Yoon, J. W.; Jhung, S. H.; Hwang, Y. K.; Humphrey, S. M.; Wood, P. T.; Chang, J. S. *Adv. Mater.* **2007**, *19*, 1830. (d) Ma, S. Q.; Wang, X.-S.; Colier, C. D.; Manis, E. S.; Zhou, H.-C. *Inorg. Chem.* **2007**, *46*, 8499. (e) Rowsell, J. C.; Yaghi, O. M. *J. Am. Chem. Soc.* **2006**, *128*, 1304. (f) Kepert, C. J. *Chem. Commun.* **2006**, 695.

(5) (a) Nouar, F.; Eubank, J. F.; Bousquet, T.; Wojtas, L.; Zaworotko, M. J.; Eddaoudi, M. *J. Am. Chem. Soc.* **2008**, *130*, 1833. (b) Hou, L.; Lin, Y.-Y.; Chen, X.-M. *Inorg. Chem.* **2008**, *47*, 1346. (c) Wong-Foy, A. G.; Lebel, O.; Matzger, A. J. *J. Am. Chem. Soc.* **2007**, *129*, 15740. (d) Lee, B. J. Y.; Olson, D. H.; Pan, L.; Emge, T. J.; Li, J. *Adv. Funct. Mater.* **2007**, 1255. (e) Lin, X.; Jia, J.; Zhao, X.; Thomas, K. M.; Blake, A. J.; Walker, G. S.; Champness, N. R.; Hubberstey, P.; Schröder, M. *Angew. Chem., Int. Ed.* **2006**, *45*, 7358. (f) Chen, B.; Ockwig, N. W.; Millward, A. R.; Contreras, D. S.; Yaghi, O. M. *Angew. Chem., Int. Ed.* **2005**, *44*, 4745.

Published on Web 11/24/2010

as the organic building block for the following purposes: (1) There were only a few reports of porous MOFs that were constructed via tetrazole functionalized aromatic carboxylic acids.[5a,6] (2) The ligand comprised multiple coordinated groups which was suitable for building extended and highly connected frameworks. (3) H_2**L** was easy to synthesize with cheap starting material in a good yield. Herein, we present a new 3D porous MOF constructed by the assembly of the $[Cu_2(O_2C)_4]$ paddle wheel unit and $\mathbf{L}^{2-}$, namely $\{[Cu\mathbf{L}]\cdot DMF\cdot H_2O\}_\infty$ (**1**) (**L** = 5-(1H-tetrazol-1-yl)isophthalic acid anion; DMF = *N*,*N*-dimethylformamide), with a rutile-related type net topology which is rare in porous MOFs. Importantly, compound **1** can be desolvated to afford a porous framework [Cu**L**] (**1a**) with 1D channels, which exhibits gas-sorption capabilities for N_2, O_2, H_2, CO_2, and CH_4 gases.

Experimental Section

Materials and General Methods. All the solvents and reagents for synthesis were obtained commercially and used as received. The ligand 5-(1H-tetrazol-1-yl)isophthalic acid was synthesized by a similar method according to the literature.[7] Infrared (IR) spectra were measured on a TENSOR 27 OPUS (Bruker) Fourier transform infrared (FT-IR) spectrometer using KBr disks dispersed with sample powders in the 4000−400 cm^{-1} range. Elemental analyses (C, H, and N) were performed on a Perkin-Elmer 240C analyzer. Thermogravimetric (TG) analyses were carried out on a Rigaku standard TG-DTA analyzer with a heating rate of 10 °C min^{-1} from ambient temperature to 800 °C; an empty Al_2O_3 crucible was used as reference.

Synthesis of $\{[CuL]\cdot DMF\cdot H_2O\}_\infty$ (1). A mixture of $CuCl_2\cdot 4H_2O$ (41 mg, 0.2 mmol) and H_2**L** (47 mg, 0.2 mmol) in DMF/MeOH (4:1 v/v) solution (15 mL) was stirred at 80 °C for 10 min and then filtered. The filtrate was kept in a beaker at room temperature. Green block-shaped crystals formed after about 1 week, were washed with DMF, and were dried in air. Yield (~60% based on H_2**L**). This material is almost insoluble in common solvents, even in DMF. Anal. Calcd (%) for $C_{12}H_{13}CuN_5O_6$: C, 37.26; H, 3.39; N, 18.11. Found (%): C, 36.89; H, 3.52; N, 17.92. IR (KBr pellet, cm^{-1}): 3071m, 2928w, 1657vs, 1595m, 1457w, 1438m, 1388vs, 1231w, 1182w, 1162w, 1090m, 996w, 916m, 782m, 746m, 729s, 660w, 492m.

X-ray Crystallography. Single crystal X-ray diffraction measurement for **1** was carried out on a Bruker Smart 1000 CCD diffractometer equipped with a graphite crystal monochromator situated in the incident beam for data collection at 113(2) K. The determinations of unit cell parameters and data collections were performed with Mo Kα radiation (λ = 0.71073 Å), and unit cell dimensions were obtained with least-squares refinement. The program SAINT[8] was used for integration of the diffraction profiles. Semiempirical absorption corrections were applied using SADABS program. The structure was solved by direct methods using the SHELXS program of the SHELXTL package and refined with SHELXL.[9] Copper atoms were found from *E*-maps, and other nonhydrogen atoms were located in successive difference Fourier syntheses. The final refinement was performed by full matrix least-squares methods with anisotropic thermal parameters for nonhydrogen atoms on F^2. The hydrogen atoms were added theoretically, riding on the concerned atoms and refined with fixed thermal factor except for H_2O molecules. Crystallographic data and experimental details for structural analyses are summarized in Table S1 (see Supporting Information). CCDC-773959 contains the supplementary crystallographic data of complex 1. These data can be obtained free of charge from the Cambridge Crystallographic Data Centre via www.ccdc.cam.ac.uk/data request/cif.

Sorption Measurements. Gas sorption experiments were carried out with a Micrometrics ASAP2020 M volumetric gas sorption instrument. Before the measurement, the sample of **1** was soaked in dichloromethane (CH_2Cl_2) for 3 days to remove DMF and H_2O solvent molecules, then filtrated, and dried at room temperature. Then, the sample was loaded in a sample tube and dried under high vacuum (less than 10^{-5} Torr) at 85 °C overnight to remove CH_2Cl_2 and all residue solvents in the channels. About 80 mg of the desolvated sample was used for the entire adsorption measurement. The hydrogen sorption isotherms were collected in a pressure range from 10^{-4} to 1 atm at 77 K in a liquid nitrogen bath and 87 K in a liquid argon bath, respectively. The O_2 isotherm measurement was also proceeded at 77 K. The gas sorption experiments of CO_2 and CH_4 were carried out at 195 K in a dry ice−acetone bath, at 273 K in an ice−water bath, and at 298 K in a temperature controlled circular bath, respectively.

Results and Discussion

Crystal Structure Description. Single-crystal structure analysis reveals that **1** crystallizes in the monoclinic system $P2_1/c$ space group. In **1**, there exists only one crystallographic independent Cu(II) center which adopts a square pyramidal coordination geometry. It is coordinated by four carboxylate O atoms from four $\mathbf{L}^{2-}$ ligands and one tetrazolyl N atom from another $\mathbf{L}^{2-}$ ligand. As shown in Figure 1a, the two adjacent Cu(II) ions are bonded together to generate a paddle wheel-shaped $\{Cu_2(O_2C)_4\}$ unit with Cu···Cu distance being 2.674 Å and Cu−O average bond length of 1.969(8) Å. The axial sites of such paddle wheel unit were occupied by the N atoms of tetrazolyl from two different $\mathbf{L}^{2-}$ ligands with the Cu−N bond length being 2.174(8) Å. As expected, the axial-assistant ligands (typically H_2O, DMF, NO_3^-, or others) in many usual MOFs with similar paddle wheel cluster units[5a,6a,10] were successfully replaced by the N-donor of tetrazolyl in the ligand, and such axial coordination mode is scarce.[6c] In the structure of **1**, each Cu_2 cluster extended by six $\mathbf{L}^{2-}$ ligands gives rise to a six-connected octahedral $[Cu_2(O_2C)_4(N)_2]$ SBU, while each $\mathbf{L}^{2-}$ anion bridges three different Cu_2 clusters serving as a three-connected triangular building block (Figure 1b). Thus, the overall structure could be described as an infinite 3D rutile-related topology (3,6)-connected framework (Figure 1c) with Schlafli symbol $(4\cdot6^2)_2(4^2\cdot6^8\cdot8^5)$ (Figure 1d). So far as we know, though (3, 6)-connected topologies have been observed in some related materials,[6b,10c,11] there was no report of the same

(6) (a) Chun, H.; Seo, J. *Inorg. Chem.* **2009**, *48*, 9980. (b) Yang, W. B.; Lin, X.; Jia, J. H.; Blake, A. J.; Wilson, C.; Hubberstey, P.; Champness, N. R.; Schröder, M. *Chem. Commun.* **2008**, 359. (c) Jia, J. H.; Lin, X.; Wilson, C.; Blake, A. J.; Champness, N. R.; Hubberstey, P.; Walker, G.; Cussena, E. J.; Schröder, M. *Chem. Commun.* **2007**, 840. (d) Zou, Y.; Hong, S.; Park, M.; Chun, H.; Lah, M. S. *Chem. Commun.* **2007**, 5182. (e) Lin, X.; Blake, A. J.; Wilson, C.; Sun, X. Z.; Champness, N. R.; George, M. W.; Hubberstey, P.; Mokaya, R.; Schröder, M. *J. Am. Chem. Soc.* **2006**, *128*, 10745.

(7) Voitekhovich, S. V.; Vorobév, A. N.; Gaponik, P. N.; Ivashkevich, O. A. *Chem. Heterocycl. Compd.* **2005**, *41*, 999.

(8) Sheldrick, G. M. *SADABS: Program for Expirical Absorption Correction of Area Detector Data*; University of Göttingen: Göttingen, Germany, 1996.

(9) Sheldrick, G. M. *SHELXTL Version 5.1. Program for Solution and Refinement of Crystal Structures*; University of Göttingen: Göttingen, Germany, 1997.

(10) (a) Yang, W. B.; Lin, X.; Blake, A. J.; Wilson, C.; Hubberstey, P.; Champness, N. R.; Schröder, M. *Inorg. Chem.* **2009**, *48*, 11067. (b) Ambrogio, M.; Fillinger, J. A.; Parkin, S.; Zhou, H.-C. *J. Am. Chem. Soc.* **2007**, *129*, 1858. (c) Sun, D. F.; Ma, S. Q.; Ke, Y. X.; Collins, D. J.; Zhou, H.-C. *J. Am. Chem. Soc.* **2006**, *128*, 3896.

(11) (a) Xie, L. H.; Liu, S. X.; Gao, B.; Zhang, C. D.; Sun, C. Y.; Li, D. H.; Su, Z. M. *Chem. Commun.* **2005**, 2402. (b) Qin, C.; Wang, X.-L.; Wang, E.-B.; Su, Z.-M. *Inorg. Chem.* **2005**, *44*, 7122. (c) Jensen, P.; Price, D. J.; Batten, S. R.; Moubaraki, B.; Murray, K. S. *Chem.−Eur. J.* **2000**, *6*, 3187.

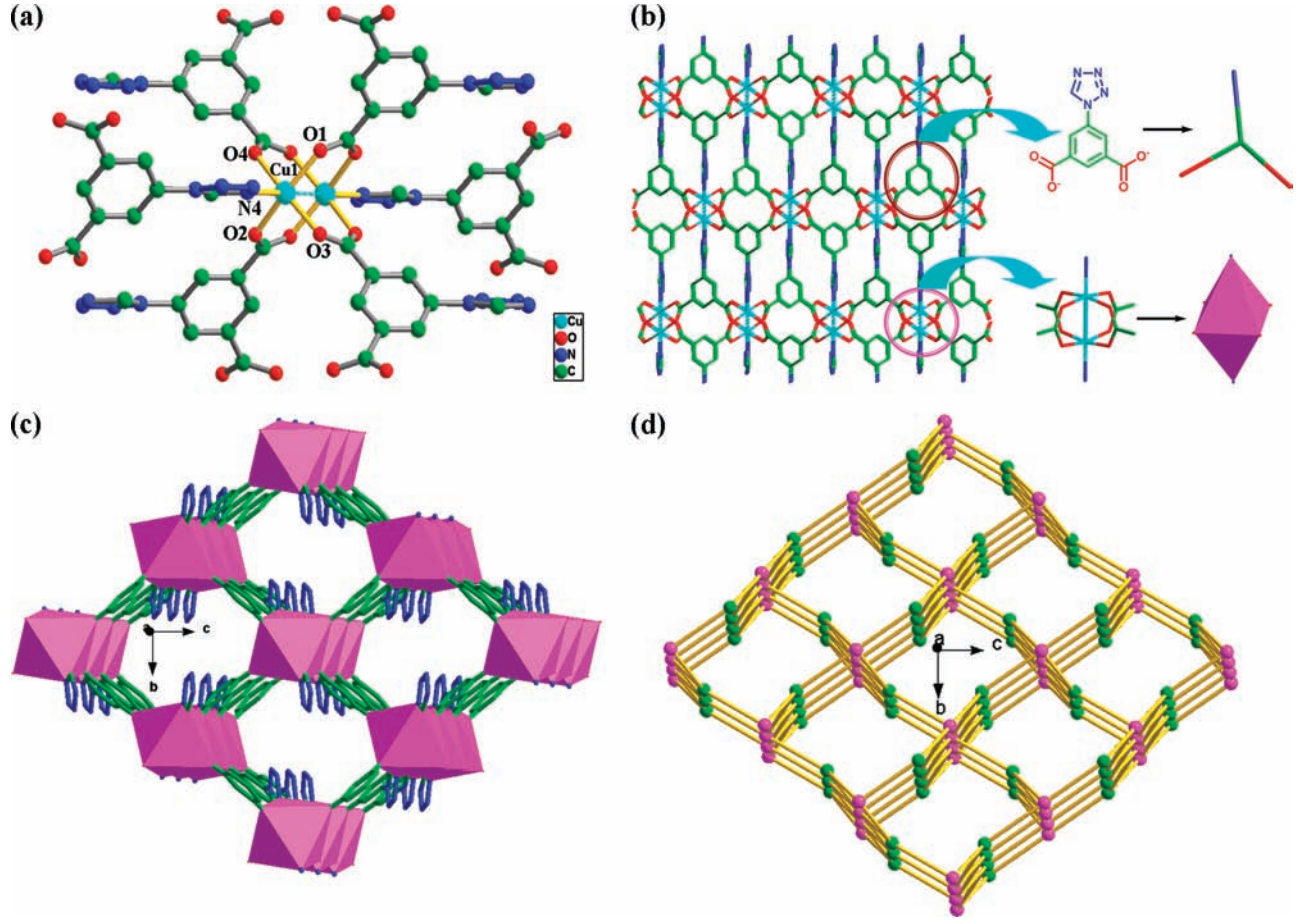

Figure 1. (a) Coordination environment of the Cu_2 dimer. (b) 2D network on *ac* plane, schematic representation of the tribranched ligand $\mathbf{L}^{2-}$, and the localized geometry of the six-connected octahedral Cu_2 unit. (c) 3D framework showing open 1D channels along the *a* axis (H atoms and solvent molecules omitted for clarity). (d) Schematic representation of the (3,6) topological net; the purple balls represent six-connected Cu_2 nodes, and green balls represent the three-connected ligand $\mathbf{L}^{2-}$.

topology for 3D frameworks constructed by N-heterocycle aromatic carboxylic acid.

In **1**, the rhombic apertures were created with phenyl rings acting as walls and $[Cu_2(O_2C)_4(N)_2]$ SBUs serving as corners (Figure 1c). Looking from the *bc* plane, the rhombic apertures assigned along *a* axis form 1D channels which were filled with DMF and H_2O solvent molecules. In addition, the tetrazolyl rings which are located at the diagonal sites of the rhombic apertures block part of the channels, while DMF molecules are located at corners and H_2O molecules are situated in the middle (Figure S1, see Supporting Information). Remarkably, the free void volume of **1** estimated by PLATON[12] is 52.1% of the total volume when the guest molecules are removed. Compared with some porous MOFs,[2e,6d,13] which were constructed by similar size organic ligands, such free void volume is fairly large.

TGA and XRPD. Thermogravimetric analysis of **1** as synthesized reveals a weight loss of 25.6% in the temperature range of 127−218 °C, which corresponds to the loss of solvent molecules residing in the open channels, one H_2O and one DMF per formula unit (calcd 23.7%). Samples after solvent exchange and vacuum activation show a similar weight loss curve, which indicated the good stability of the framework after the removal of solvent molecules (Figure S2, see Supporting Information). The X-ray powder diffraction (XRPD) pattern of solid **1** is coincident with the simulated pattern derived from the X-ray single crystal data, implying that the bulk sample is the same as the single crystal (Figure 2). Prior to gas-sorption experiments, DMF and H_2O molecules were removed from compound **1** by solvent exchange. The solvent exchanged sample was then dried under high vacuum to get the desolvated solid [Cu**L**] (**1a**). The activated sample **1a** is still crystalline, as evidenced by the XRPD patterns (Figure 2). Though the experimental patterns of the activated sample show few unindexed and slightly broadened diffraction lines, which might be attributed to the slight change of structure caused by the removal of guest molecules, the whole porous framework should remain.

Adsorption Properties. Gas-sorption experiments of the desolvated solid [Cu**L**] (**1a**) were carried out for N_2, H_2, O_2, CH_4, and CO_2 gases to examine the porous properties and its gas storage capability. The results of gas adsorption for **1a** are listed in Table 1.

To investigate the porosity of **1a**, N_2 sorption was performed at 77 K. The uptake amount of N_2 is 255 ± 3 cm^3/g (STP) at 1 atm, and the gas sorption shows a reversible

(12) Spek, A. L. *PLATON, A Multipurpose Crystallographic Tool*; Utrecht University: Utrecht, The Netherlands, 2006.

(13) (a) Qiu, Y. C.; Deng, H.; Yang, S. H.; Mou, J. H.; Daiguebonne, C.; Kerbellec, N.; Guillou, O.; Batten, S. R. *Inorg. Chem.* **2009**, *48*, 3976. (b) Li, C.-J.; Lin, Z.-J.; Peng, M.-X.; Leng, J.-D.; Yang, M.-M.; Tong, M.-L. *Chem. Commun.* **2008**, 6348.

Table 1. Gas-Adsorption Data for **1a**

gas	temperature and pressure	amount of gas adsorb		
		wt %	cm^3/g	mmol/g
N_2	77 K and 0.2 atm/1 atm	30.0/31.9	240 ± 2/255 ± 3	10.7/11.4
O_2	77 K and 0.2 atm	38.8	272 ± 2	12.1
H_2	77 K and 0.2 atm/1 atm	1.37/1.86	153 ± 3/208 ± 4	6.83/9.28
	87 K and 1 atm	1.51	169 ± 2	7.54
CO_2	195 K	37.7	192 ± 2	8.57
	273 K	29.7	151 ± 3	6.74
	298 K	21.8	111 ± 2	4.95
CH_4	195 K (1 atm)	8.50	119 ± 2	5.31
	273 K	3.14	44 ± 2	1.96
	298 K	1.64	23 ± 2	1.03

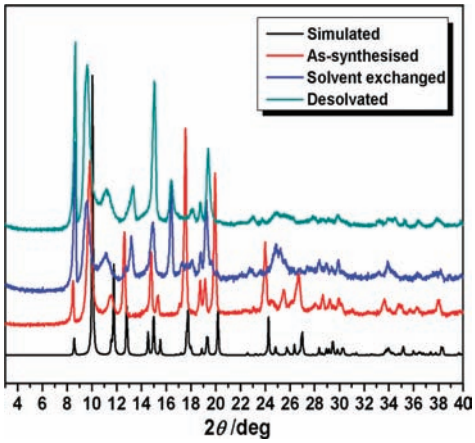

Figure 2. XRD powder patterns for compounds **1** (red) and **1a** (green).

type I isotherm with a slightly hysteresis on desorption (Figure 3a), being characteristic of the microporous material. The Brunaer-Emmett-Teller (BET) and Langmuir surface area of guest-free framework are estimated to be 810 and 1063 m^2/g, respectively, and the H−K (Horvath−Kawazoe)[14] pore diameter is 7.9 Å. Furthermore, the H−K pore volume is 0.34 cm^3/g, a little lower than the value of 0.35 cm^3/g calculated from the crystal structure, which indicates that the gas molecules fill the void space efficiently.

The accessible porosity in **1a** confirmed by the N_2 sorption study prompts us to investigate further gas sorption properties of **1a**. Subsequently, the H_2 and O_2 adsorption measurements for **1a** were carried out. The H_2 sorption isotherms at 77 and 87 K both show type I behavior with no hysteresis and no noticeable change in

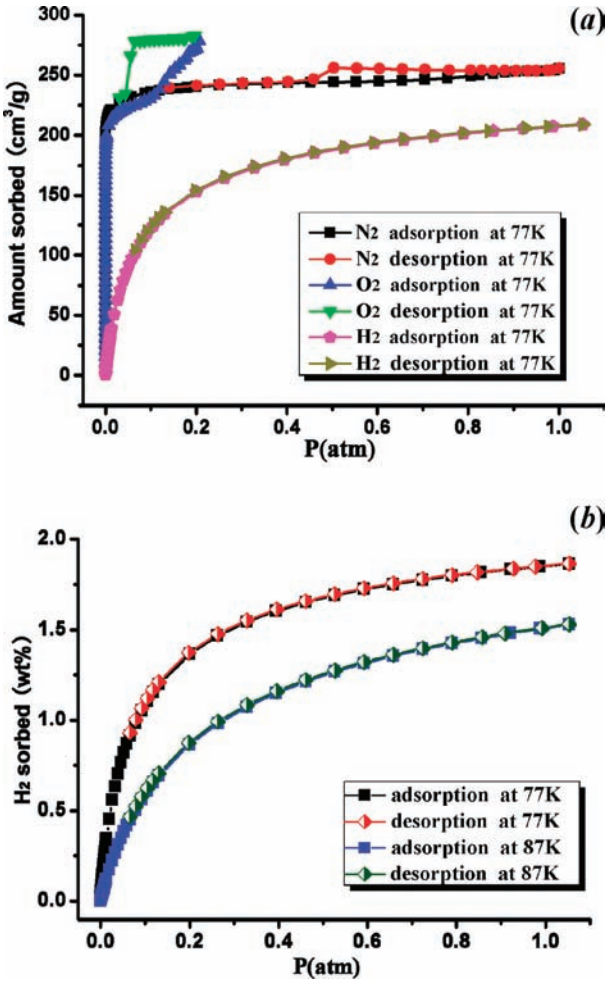

Figure 3. Gas sorption isotherms for **1a**: (a) N_2, H_2, and O_2 at 77 K and (b) H_2 at 77 and 87 K.

the properties upon repeated cycling (Figure 3b). The uptake of H_2 at 1 atm and 77 K is 1.86 wt % (208 ± 4 cm^3/g, STP), which is higher than that of many reported MOFs under the same conditions[6b,10a,15,16] but lower than some of the best MOFs.[4a,5a,e,17] However, compared with some MOFs possessing larger surface area and high porosity, such an amount of H_2 adsorption for **1a** is still inspiring (Table S2, see Supporting Information).[4a,5c,6c,10b,c] For example, the MOF $[Fe_3(O)(L_1)_3]$[6c] (H_2L_1 = pyridine-3,5-bis (phenyl-4-carboxylic acid)) with a BET area of 1200 m^2/g, but the uptake of H_2 at 1 atm and 77 K, is 1.60 wt %; the PCN-6′[10b] with Langmuir area being 2700 m^2/g and the uptake of H_2 at 1 atm and 77 K is only ~1.62 wt %.

(14) (a) Horvath, G.; Kawazoe, K. J. *Chem. Eng. Jpn.* **1983**, *16*, 470. (b) Hou, L.; Lin, Y.-Y.; Chen, X.-M. *Inorg. Chem.* **2008**, *47*, 1346.
(15) (a) Guo, Z. Y.; Li, G. H.; Zhou, L.; Su, S. Q.; Lei, Y. Q.; Dang, S.; Zhang, H. J. *Inorg. Chem.* **2009**, *48*, 8069. (b) Lan, A. J.; Li, K. H.; Wu, H. H.; Kong, L. Z.; Nijem, N.; Olson, D. H.; Emge, T. J.; Chabal, Y. J.; Langreth, D. C.; Hong, M. C.; Li, J. *Inorg. Chem.* **2009**, *48*, 7165. (c) Pan, L.; Parker, B.; Huang, X. Y.; Olson, D. H.; Lee, J. Y.; Li, J. *J. Am. Chem. Soc.* **2006**, *128*, 4180.
(16) (a) Yu, Q.; Zeng, Y.-F.; Zhao, J.-P.; Yang, Q.; Hu, B.-W.; Chang, Z.; Bu, X.-H. *Inorg. Chem.* **2010**, *49*, 4301. (b) Ma, S. Q.; Yuan, D. Q.; Wang, X.-S.; Zhou, H.-C. *Inorg. Chem.* **2009**, *48*, 2072. (c) Eun Cheon, Y.; Park, J.; Paik Suh, M. *Chem. Commun.* **2009**, 5436. (d) Neofotistou, E.; Malliakas, C. D.; Trikalitis, P. N. *Chem.—Eur. J.* **2009**, *15*, 4523.
(17) (a) Wang, X.-S.; Ma, S. Q.; Forster, P. M.; Yuan, D. Q.; Eckert, J.; López, J. J.; Murphy, B. J.; Parise, J. B.; Zhou, H.-C. *Angew. Chem., Int. Ed.* **2008**, *47*, 7263. (b) Latroche, M.; Surble, S.; Serre, C.; Mellot-Draznieks, C.; Llewellyn, P. L.; Lee, J.-H.; Chang, J.-S.; Jhung, S. H.; Férey, G. *Angew. Chem., Int. Ed.* **2006**, *45*, 8227. (c) Panella, B.; Hirscher, M.; Putter, H.; Muller, U. *Adv. Funct. Mater.* **2006**, *16*, 520.

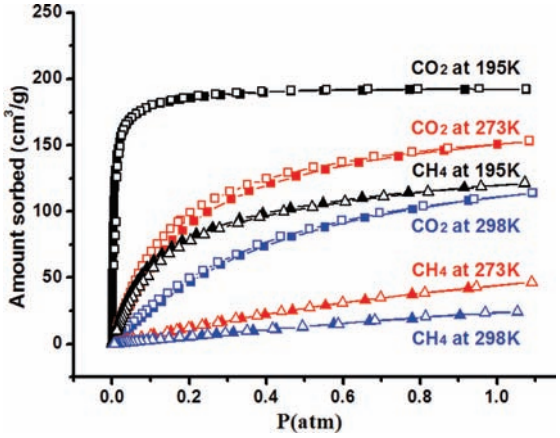

Figure 4. Gas sorption isotherms of CO_2 (square) and CH_4 (triangle) for **1a**, at 195 K (black), 273 K (red), and 298 K (blue), respectively. (Filled shapes represent adsorption, and open shapes represent desorption.)

Moreover, the hydrogen isosteric heats of adsorption (Q_{st}) for **1a** calculated from the respective adsorption isotherms at 77 and 87 K, employing the Clausius−Clapeyron equation,[18] are 7.2−6.8 kJ·mol^{-1} depending on the degree of H_2 loading (Figure S4, see Supporting Information), which is in the usual range of the porous MOFs (Table S4, see Supporting Information).[3a,b,4c,19] The approximate value of 7.2 kJ·mol^{-1} at zero surface coverage obtained from isotherm studies is close to the corresponding values found for most promising MOFs for hydrogen storage.[4a,20]

In the case of O_2 adsorption, **1a** adsorbs up to 38.7 wt % (272 ± 2 cm^3·g^{-1}, 12.1 mmol·g^{-1}, STP) at 77 K and 0.19 atm, far higher than that of H_2 gas under the same condition (Figure 4a). Such O_2 capacity is also very high compared with many other porous MOFs (Table S3, see Supporting Information).[3a,4b,16b,c,21] Notably, the O_2 isotherm has two adsorption steps with more marked hysteresis than that of N_2 on desorption (Figure S5, see Supporting Information). In the first step interval from 0 to 0.6 of P/P_0, the saturation plateau occurs and the monolayer coverage predicted by fitting Langmuir equations to the N_2 and O_2 isotherms are almost identical (10.93 and 10.91 mmol·g^{-1} at the relative pressure of 0.6, respectively), suggesting that the same number of binding sites is initially available to both gases.[21] The second step occurs in the relative pressure P/P_0 interval 0.6−0.93 and corresponds to adsorption of ca. 12.1 mmol·g^{-1} of O_2, a little higher than that of N_2 gas (255 ± 3 cm^3·g^{-1}, 11.3 mmol·g^{-1}, STP). Such behavior may be attributed to the multilayer adsorption or the multiple MOF−adsorbate interactions with different intensity.[3a] Although hysteresis is observed between the adsorption and desorption curves, O_2 uptake in **1a** is reversible (Figure S3, Supporting Information), suggesting that O_2 does not permanently bind to the framework via an irreversible process such as oxidation of the metal centers.[21] The O_2 adsorption density in **1a**, as estimated by the H−K pore volume (0.34 cm^3·g^{-1}) measured using the N_2 isotherm, is 1129 kg·m^{-3} at 0.19 atm which suggests that O_2 gas is highly compressed within the pores (the density of liquid O_2 is 1140 kg·m^{-3}) and it is a high value among those of reported porous MOFs.[3a,4b,16b,c] Since **1a** shows high uptake of O_2 and selective sorption of O_2 over H_2 and N_2 over H_2, it may have potential application in the separation of these gases at low pressure.

Although most adsorption studies on porous materials have been carried out for hydrogen storage purpose in the past few years, there are now increasing investigations aimed at different objectives for other gases, such as O_2, CO_2, CH_4, etc.[2b,4a,16b,21,22] To further check the gas adsorption properties of **1a**, CO_2 and CH_4 adsorption studies have been systematically carried out, at 195, 273, and 298 K under normal pressure, respectively. All the adsorption isotherms exhibit typical type I sorption behavior (Figure 4), and the adsorption capacities of CO_2 are higher than that of CH_4 under the same condition. It is noteworthy that the adsorption quantities are superior to those of most related MOFs measured under similar conditions (Table S3, see Supporting Information),[3a,6a,22] although lower than those of some of the best MOFs.[4a,13b,23] At 1 atm and 195 K, **1a** adsorbs CO_2 gas up to 192 ± 2 cm^3·g^{-1} (STP), while the adsorbed amount of CH_4 is 119 ± 2 cm^3·g^{-1} (STP) which is even lower than that of CO_2 (151 ± 3 cm^3·g^{-1} at STP) at 1 atm and 273 K, indicating the high selectivity of gas sorption for CO_2 over CH_4. Furthermore, such selectivity is more and more remarkable along with the temperature increasing (Figure S6, see Supporting Information, and Table 1). It may mainly be attributed to two factors: (1) The kinetic diameter of the CO_2 molecule (3.3 Å) is smaller than that of the CH_4 molecule (3.8 Å),[24] and access to the channels in **1a** is easier. (2) The quadrupole moment of CO_2 (-1.4×10^{-39} C m^2) might induce stronger interaction with the porous framework than CH_4.[3a,15b,25]

Most interestingly, although the CO_2 uptakes of some excellent MOFs are higher than that of **1a** at 195 K and normal pressure, the values for them at 273 or 298 K are lower than those of **1a** (37.7 wt % at 195 K, 29.7 wt % at 273 K, and 21.8 wt % at 298 K) under the same condition. For example, $[Zn_2(abtc)(dmf)_2]_3$ is 55.1 wt % at 195 K (but 20.6 wt % at 273 K),[4a] $[\{Cu_2(abtc)(dmf)_2\}_3]$ is 53.8 wt % at 195 K (but 19.2 wt % at 273 K),[4a] and the desolvated solid of $[Cu_{24}\mathbf{L}_{12}(DMF)_8(H_2O)_{16}]$ is ~84.8 wt % at 196 K (but ~19.6 wt % at 298 K).[23] It is noteworthy that **1a** still shows a high CO_2 adsorption amount of 21.8 wt % (4.95 mmol·g^{-1}, 111 ± 2 cm^3·g^{-1}, STP) at ambient temperature (298 K) and 1 atm, which is remarkably high compared with the corresponding values of many representative porous MOFs (Table S3, see Supporting Information).[3c,13,23] Similar adsorption results were obtained for CH_4, indicating the excellent capability of **1a** in the sorption of CO_2 and CH_4 at normal temperature and pressure. Since the efficient separation of CO_2 from air under atmospheric pressure has become an important

(18) Yang, R. T. *Gas Adsorption by Adsorption Processes*; Butterworth: Boston, 1997.
(19) (a) Dinca, M.; Long, J. R. *Angew. Chem., Int. Ed.* **2008**, *47*, 6766. (b) Zhou, W.; Wu, H.; Yildirim, T. *J. Am. Chem. Soc.* **2008**, *130*, 15268.
(20) Rowsell, J. L. C.; Yaghi, O. M. *J. Am. Chem. Soc.* **2006**, *128*, 1304.
(21) Dincă, M.; Yu, A. F.; Long, J. R. *J. Am. Chem. Soc.* **2006**, *128*, 8904.
(22) Mu, B.; Li, F.; Walton, K. S. *Chem. Commun.* **2009**, 2493.
(23) Liu, X. F.; Park, M.; Hong, S.; Oh, M.; Yoon, J. W.; Chang, J.-S.; Soo Lah, M. *Inorg. Chem.* **2009**, *48*, 11507.
(24) Beck, D. W. *Zeolite Molecular Sieve*; Wiley & Sons: NewYork, 1974.
(25) (a) Coriani, S.; Halkier, A.; Rizzo, A.; Ruud, K. *Chem. Phys. Lett.* **2000**, *326*, 269. (b) Bae, Y.-S.; Mulfort, K. L.; Frost, H.; Ryan, P.; Punnathanam, S.; Broadbelt, L. J.; Hupp, J. T.; Snurr, R. Q. *Langmuir* **2008**, *24*, 8592.

issue for both science and industry,[6a,26] compound **1a** may be of potential use for CO_2 gas separation or purification.

Conclusion

In summary, we have prepared a new metal−organic framework with paddle wheel-shaped SBU $[Cu_2(O_2C)_4(N)_2]$ without any assistant ligand at the axial site and demonstrated its gas sorption properties of N_2, O_2, H_2, CO_4, and CH_4. The results exhibit selective gas sorption properties of **1a** for O_2 over H_2 and high selectivity for CO_2 over CH_4, indicating its potential applications in gas separation. Furthermore, its excellent O_2 uptake at 77 K and remarkably high quantity of adsorption for CO_2 at room temperature (298 K) and atmospheric pressure may be of use for gas separation or purification.

Acknowledgment. This work was financially supported by the 973 Program of China (2007CB815305), the NNSF of China (21031002 and 20801029), and the Natural Science Fund of Tianjin, China (10JCZDJC22100).

Supporting Information Available: X-ray crystallographic files in CIF format for **1**, TGA curve, and some graphics, Table S1 crystal data and structure refinement for compound **1**, Tables S2−S4 summary of gases adsorption data for related MOFs in recent literature. This material is available free of charge via the Internet at http://pubs.acs.org.

(26) (a) Caskey, S. R.; Wong-Foy, A. G.; Matzger, A. J. *J. Am. Chem. Soc.* **2008**, *130*, 10870. (b) Banerjee, R.; Phan, A.; Wang, B.; Knobler, C.; Furukawa, H.; O'Keeffe, M.; Yaghi, O. M. *Science* **2008**, *319*, 939. (c) Broecker, W. S. *Science* **2007**, *315*, 1371. (d) Marris, E. *Nature* **2006**, *442*, 624. (e) Llewellyn, P. L.; Bourrelly, S.; Serre, C.; Filinchuk, Y.; Férey, G. *Angew. Chem., Int. Ed.* **2006**, *45*, 7751.